JACS
JOURNAL OF THE AMERICAN CHEMICAL SOCIETY
Article
pubs.acs.org/JACS

Molecular Donor–Bridge–Acceptor Strategies for High-Capacitance Organic Dielectric Materials

Henry M. Heitzer, Tobin J. Marks,* and Mark A. Ratner*

Department of Chemistry and the Materials Research Center, Northwestern University, 2145 Sheridan Road, Evanston, Illinois 60208, United States

ABSTRACT: Donor–bridge–acceptor (DBA) systems occupy a rich history in molecular electronics and photonics. A key property of DBA materials is their typically large and tunable (hyper)polarizabilities. While traditionally, classical descriptions such as the Clausius–Mossotti formalism have been used to relate molecular polarizabilities to bulk dielectric response, recent work has shown that these classical equations are inadequate for numerous materials classes. Creating high-dielectric organic materials is critically important for utilizing unconventional semiconductors in electronic circuitry. Employing a plane-wave density functional theory formalism, we investigate the dielectric response of highly polarizable DBA molecule-based thin films. Such films are found to have large dielectric response arising from cooperative effects between donor and acceptor units when mediated by a conjugated bridge. Moreover, the dielectric response can be systematically tuned by altering the building block donor, acceptor, or bridge structures and is found to be nonlinearly dependent on electric field strength. The computed dielectric constants are largely independent of the density functional employed, and qualitative trends are readily evident. Remarkably large computed dielectric constants >15.0 and capacitances >6.0 μF/cm^2 are achieved for squaraine monolayers, significantly higher than in traditional organic dielectrics. Such calculations should provide a guide for designing high-capacitance organic dielectrics that should greatly enhance transistor performance.

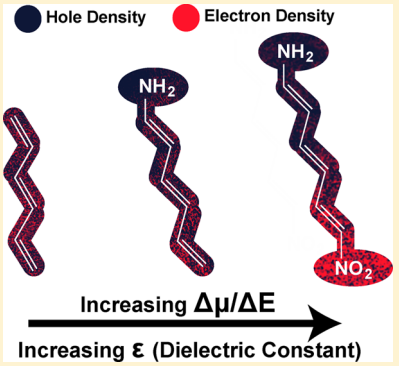

INTRODUCTION

The field of organic electronics has recently experienced tremendous growth and research intensity. The attraction lies in possibility of mass producing high-performance flexible products for communication, displays, sensing, and ultimately the "internet of things" at low cost.[1−3] In the case of organic field effect transistors (OFETs), organic materials can be used for both the semiconductor and gate dielectric components. Extensive research has focused on enhancing the carrier mobility, on/off ratio, and other metrics in organic semiconducting materials by varying the structural and electronic properties as well as film growth processes.[4−12] While some design principles associated with the performance of organic dielectrics have been elucidated, this area is at a far earlier stage of development.[13−22] Goals for enhancing organic dielectric performance must include increasing the capacitance, to lower OFET operating voltages while preserving insulating characteristics. To date, most approaches to achieve these ends have been highly empirical and have met with limited success. This contribution focuses on first-principles computational approaches to guide the design of new classes of thin-film organic gate dielectrics, focusing on what is identified here as a particularly promising class of thin-film materials, donor–bridge–acceptor (DBA) molecular monolayers.

Traditionally, organic materials are characterized by low dielectric constants, ε, in solid-state systems (ε = 2.0–4.0).[23,24] While small dielectric constants may prohibit most organic materials from achieving high capacitances, recent developments in device fabrication have made it possible to create OFET-quality monolayer or multilayer dielectric films of small organic molecules.[13,19,22−28] At sufficient thinness, $d \leq 5.0$ nm, organic monolayers can exhibit appreciable capacitances, C, >1.0 μF/cm^2.[13,27,29] While substantial work has been devoted to making thinner materials, only a few studies have focused on rationally increasing the dielectric constant.[13,14,16,18,22,30]

Dielectric responses in organic materials have frequently been modeled using the Clausius–Mossotti[31] relationship (eq 1) relating the dielectric constant, ε, to the polarizability, α, and N, the number of molecules per unit volume.[21] However, recent work has revealed the limitations of (eq 1) for computing dielectric responses in organic materials:[32−34]

$$\varepsilon = \frac{3 + 2(4\pi N)\alpha}{3 - (4\pi N)\alpha} \quad (1)$$

The limitations of the Clausius–Mossotti formalism are rooted in the relationship of a molecular property (polarizability) to a bulk materials property (dielectric constant). Polarizability in a film is greatly overestimated in standard, small-molecule, quantum calculations, leading to overestimations of the dielectric response.[33] Treating the dielectric response as a property of the constituent molecules ignores that fact that the response can be critically dependent on molecular orientations and can exhibit large anisotropy for different materials densities and conformations.[16,32] These considerations illustrate the need

Received: March 30, 2015
Published: May 15, 2015

DOI: 10.1021/jacs.5b03301
J. Am. Chem. Soc. 2015, 137, 7189–7196

for a capability to carry out reliable dielectric computations on bulk, periodic molecular systems. By introducing periodic boundary conditions, molecular density and orientation effects on the dielectric response can thereby be accounted for. While such an approach has been applied successfully to hard matter dielectrics,[35−38] only recently has this treatment been applied to molecular systems.

The inherent limitations of using the Clausius−Mossotti description to relate polarizability to dielectric constant do not preclude it from being a useful tool for understanding qualitative trends in molecular materials. Previous work has shown that materials with large (hyper)polarizabilities generally exhibit significantly higher dielectric responses than other molecular materials.[21,39,40] In this regard, electron-donating and electron-accepting moieties are known to enhance molecular (hyper)polarizabilities when introduced in tandem to conjugated π-systems.[41−44] These molecular materials, commonly referred to as DBA materials (Figure 1) have inspired

Figure 1. DBA molecular architecture.

significant research in the scientific community for implementation in nonlinear optics,[44−47] charge transfer,[48−50] and charge transport.[51,52] In this contribution, we investigate DBA motif molecular monolayers for applications in high-capacitance organic dielectrics, using first-principles density functional theory (DFT) in combination with periodic boundary conditions. By analyzing structure−function relationships in DBA materials, we are able to suggest new molecular dielectric materials that attain a very large, calculated $\varepsilon > 15.0$ and $C > 6.0$ μF/cm^2.

METHODS

Utilizing techniques outlined in a previous study of far simpler systems,[32,33] dielectric constants for monolayer films are computed using a finite difference approach. To begin, a single molecule is placed in a periodic unit cell of dimensions x, y, and z as shown in Figure 2. Although only a single molecule is modeled, the periodic boundary conditions imposed replicate a square-symmetric monolayer film. The x and y dimensions describe surface coverage of the molecular

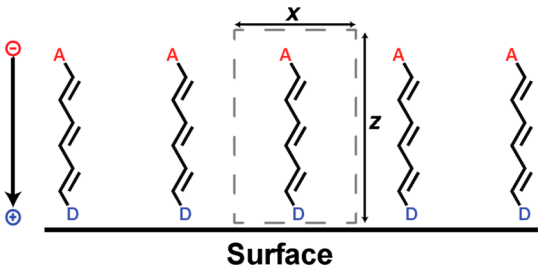

Figure 2. Schematic representation of first-principles computation of the dielectric response of a DBA molecular monolayer film on a surface. The unit cell, indicated by the gray dashed box, contains one molecule that is replicated using periodic boundary conditions. The unit cell dimensions x and y determine the molecular density of the modeled film. Note that the y dimension is perpendicular to the xz plane. The z dimension represents the thickness of the monolayer and is at least 15 Å greater than the height of the molecule to ensure no interaction between monolayers. Donor and acceptor moieties are represented by D and A, respectively.

monolayer. Surface molecular density values typically range from 2.0−5.0 molecules/nm^2, depending on the interaction between the substrate and assembled monolayer and the interactions between the constituent molecules.[26,53] In this work, the surface coverage and the corresponding x and y coordinates are explicitly reported for each simulation, as they are critically important to the dielectric response. The z-axis is taken to be perpendicular to the surface and is sufficiently extended to ensure at least 15.0 Å of vacuum between monolayers so interactions between monolayers are negligible as demonstrated in our prior work.[23] Interactions between surface and substrate have been shown to have minimal and short-lived effects on the dielectric response.[38,54] For this reason we omit including an explicit surface, which would greatly add to the computational expense of the simulation. After optimizing the geometry of the molecular film, two different electric fields, E_1 and E_2, are applied separately, and the geometry is optimized in the presence of the external electric field. E_{ext} is defined as the difference between E_1 and E_2. For the majority of simulations, $E_1 = 5.14 \times 10^8$ V/m and $E_2 = -5.14 \times 10^8$ V/m, typical values for applied electric fields in devices.[21] Electric fields are applied parallel to the z-axis, simulating an electric field across a monolayer. Any electric field strength that differs from $\pm 5.14 \times 10^8$ V/m will be noted in the text.

After applying the two electric fields, the change in dipole moment is used to determine the dielectric constant via eq 2:[32,38,55]

$$\varepsilon = \frac{\varepsilon_0 E_{ext}}{\varepsilon_0 E_{ext} - P} \tag{2}$$

where ε_0 is the vacuum permittivity. The polarization for of the monolayer is defined as in eq 3:

$$P = \frac{\Delta\mu}{V_{ML}} \tag{3}$$

where $\Delta\mu$ is the change in dipole moment of the monolayer induced by an applied field, and V_{ML} is the volume of the monolayer. V_{ML} is the area of the unit cell times the thickness of the monolayer.

In this study, two different dielectric constants are examined: (1) The optical dielectric constant, ε_{opt}, represents dielectric responses at high frequency, $\omega \sim \infty$ Hz, before any geometry changes occur in the presence of the electric field, and (2) the static dielectric constant, ε_{stat}, is the limit of low-frequency dielectric response, $\omega = 0$ Hz, after geometry optimization. In both the optical and static responses, no molecular translational or rotational motion is allowed.

Dielectric calculations are performed in QUANTUMESPRESSO (QE).[56] Two different density functionals are applied in these studies. The generalized gradient approximation (GGA), as implemented by the Perdew−Burke−Ernzerhof (PBE)[57] scheme, is used to treat all systems. GGA functionals have been used in a variety of dielectric calculations, including polar and nonpolar organic multilayers,[32] phthalocyanine ribbons,[58] and metal-oxide/organic interfaces[38] and have proven accurate, typically matching experimental dielectric constants within ∼10%. It is known that GGA functionals typically overestimate polarizability in conjugated materials; therefore our calculated results likely represent upper bounds for experimental dielectric constants, but are still instructive and of useful accuracy.[59,60] The Heyd−Scuseria−Ernzerhof (HSE) screened hybrid density functional[61] is used on smaller molecules to test the accuracy of the results. It is not applied to all systems due to the large computational expense within the planewave packages. For PBE functionals, Vanderbilt ultrasoft pseudopotentials[62] are used with kinetic energy cutoff values of 60 and 660 Ry for wave functions and charge density, respectively. Forces were converged to 20 meV/Å, and a k-point scheme of $2 \times 2 \times 1$ was implemented.

In addition to calculations performed in QE, polarizability calculations were carried out using GAMESS to compare dielectric constants calculated using the traditional Clausius−Mossotti relationship and the method outlined above. A diffuse basis set, aug-cc-pVDZ, was employed with PBE to obtain polarizability values. Polarizabilities are used here for qualitative, not quantitative, analysis among different

DOI: 10.1021/jacs.5b03301
J. Am. Chem. Soc. 2015, 137, 7189−7196

molecules to identify trends. Quantitatively rigorous polarizability calculations require higher-level calculations as shown elsewhere.[63−65]

RESULTS AND DISCUSSION

Donor−Bridge−Acceptor Units. To verify the initial hypothesis that DBA systems can exhibit large dielectric constants, five different structures based on a six-carbon polyacetylene fragment were tested, as shown in Figure 3A.

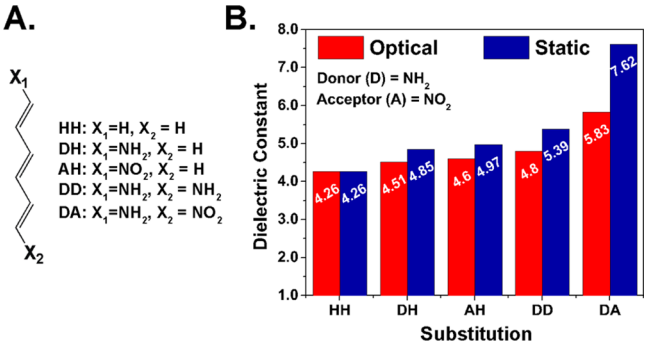

Figure 3. First-principles DFT computation of the optical and static dielectric constant of six-carbon polyacetylene self-assembled monolayers having the indicated donor and acceptor substituents. (A) Molecular structures of the component molecular building blocks with the indicated substituents. (B) Optical (red stripe) and static (blue solid) dielectric constants of the variously substituted polyacetylene-based monolayers. The unit polyacetylene cell contains one molecule and has dimensions of 5.00 × 5.00 × 30.0 Å. The applied electric fields are parallel to the z axis and have a strength of $\pm 5.14 \times 10^8$ V/m. A k-point sampling scheme of 2 × 2 × 1 is used for each material. The molecular axis is perpendicular to the surface.

Three different substituents (H, NH_2, and NO_2) are used to represent neutral, donor, and acceptor moieties, respectively. Figure 3B shows the computed optical (high frequency) and static (low frequency) dielectric constants for monolayers composed of the indicated molecules at a surface coverage of 4.0 molecules/nm^2. The smallest dielectric response arises from HH, two hydrogen atoms at locations X_1 and X_2 in Figure 3A, the optical and static dielectric constants of which are equivalent ($\varepsilon_s = \varepsilon_o = 4.26$). Without polar bonds, the HH dielectric response is solely due to electronic polarization, resulting in equivalent dielectric responses at high and low frequencies.[32] Both DH and AH exhibit larger optical and static dielectric responses than HH. The difference in optical responses results from increased electron density contributions from both NH_2 and NO_2.[66] In DH and AH, the static dielectric constant is enhanced corresponding to the introduction of polar bonds which create additional polarization. Polarization induced by geometric changes in polar bonding occurs on slower time scales than changes in electron density and includes dipolar and atomic polarization due to reorientation of dipoles and displacement of nuclei, respectively, in polar environments.[66] Similarly, DD's dielectric constant is slightly greater than DH due to the addition of another electron-rich group. Interestingly, DA has a significantly higher computed static dielectric response ($\varepsilon_s = 7.62$) than does DD ($\varepsilon_s = 5.29$). If dielectric response were strictly additive, then DD would have a nearly equivalent dielectric response since the dielectric constant of DH ≈ AH. Introducing donor and acceptor groups at opposite ends of the conjugated bridge clearly results in larger dielectric responses than predicted by individual summations, indicating cooperative enhancement. This result comports qualitatively with a Clausius−Mossotti picture since large polarizations are possible in DBA molecules,[44] leading to increased dielectric response. Since the static dielectric constant is enhanced more than the optical counterpart, it is likely that donor−acceptor interactions more strongly influence dipolar and atomic polarizations that occur on longer time scales due to constraints of atomic rearrangement processes, than electronic polarization that occurs instantaneously.

Given the rich history of DBA systems in nonlinear optics, it is of interest to examine similar phenomena for dielectric materials. Nonlinear behavior occurs when very large electric fields, $E > 10^8$ V/m, are applied.[67] In ultrathin systems, even while operating at relatively small voltages of ∼1.0 V, electric field strengths inducing nonlinear behavior are readily achievable. In HH systems, only linear response is expected, making HH a good comparison to DA, where nonlinear behavior is predicted. In Table 1, static and optical dielectric constants for HH and DA are reported at different applied fields. At all applied fields, the HH optical and static dielectric constants remain nearly invariant to the field strength. This is expected since near-centrosymmetric HH should have negligible second-order nonlinear response properties. In contrast, the DA static dielectric constant increases with stronger electric fields, indicating nonlinear dielectric behavior. Changes in dipole moment increase nonlinearly in the presence of strong electric fields as shown by Taylor series expansion of the induced dipole moment as shown in eq 4:

Table 1. Computed Static and Optical Dielectric Constants of HH and DA Monolayers at Varied Electric Field Strengths

	applied electric field strength					
	$E=5.14\times10^7$ V/m[a]		$E=5.14\times10^8$ V/m		$E = 2.57 \times 10^9$ V/m	
monolayer	ε_o[b]	ε_s[c]	ε_o	ε_s	ε_o	ε_s
HH	4.15	4.15	4.26	4.26	4.21	4.28
DA	5.73	5.75	5.83	7.62	5.87	11.07

[a]Applied electric field strength along the z axis. [b]Optical dielectric constant. [c]Static dielectric constant.

$$\mu(E) = \mu_0 + \alpha E + \frac{1}{2}\beta E^2 + \frac{1}{6}\gamma E^3 + \ldots \quad (4)$$

where α, β, and γ are the first-, second-, and third-order polarizability coefficients and E is the electric field strength. For materials, a similar expansion is found for macroscopic polarization (P) terms of susceptibility ($X^{(n)}$) coefficients as shown in eq 5:[44]

$$P(E) = P_0 + \chi^1 E + \frac{1}{2}\chi^2 E^2 + \frac{1}{6}\chi^3 E^3 + \ldots \quad (5)$$

Note that the polarizability coefficients are not functions of E and that the Clausius−Mossotti description, which uses α as the sole polarizability parameter, cannot account for nonlinear behavior. However, this deficiency is often small enough that the effect on calculated parameters is relatively minor. In principle, α can only be determined using finite difference methods when the applied electric fields are very small as in eq 6:

$$\frac{d\mu(E)}{dE} = \alpha, \quad dE \cong 0.0 \quad (6)$$

DOI: 10.1021/jacs.5b03301
J. Am. Chem. Soc. 2015, 137, 7189−7196

However, what is approximately close to 0.0 V/m can vary from molecule to molecule. To demonstrate, the calculated optical and static polarizabilities for HH and DA molecules using finite difference methods at commonly used electric field strengths are compared in Table 2. For HH, α remains nearly constant over all electric fields tested, while for DA, α increases with electric field strength.

Table 2. Static and Optical Polarizability of HH and DA at Varied Electric Field Strengths

	applied electric field strength					
	$E = 5.14 \times 10^7$ V/m[a]		$E = 5.14 \times 10^8$ V/m		$E = 2.57 \times 10^9$ V/m	
monolayer	α_o[b]	α_s[c]	α_o	α_s	α_o	α_s
HH	156.1	157.4	156.5	159.3	157.3	163.4
DA	358.5	434.6	360.2	463.2	365.5	520.2

[a]Applied electric field strength along the z axis. [b]Optical polarizability (au).[3] [c]Static polarizability (au).[3]

The polarizability α should not vary with applied electric field. Nonlinear characteristics are captured by the higher order polarizability terms β and γ. In practice, what is often calculated as α is in fact given by eq 7:

$$\frac{\Delta\mu}{\Delta E} = \frac{\mu(E_1) - \mu(E_2)}{E_1 - E_2} = \alpha + \beta(E_1 - E_2) + \frac{1}{2}\gamma(E_1 - E_2)^2 + \ldots \quad (7)$$

As commonly referenced, the Clausius−Mossotti description is valid for materials having only linear response properties. For materials with nonlinear behavior, eq 1 should be rewritten as in eq 8:

$$\varepsilon = \frac{3 + 2(4\pi N)\frac{\Delta\mu}{\Delta E}}{3 - (4\pi N)\frac{\Delta\mu}{\Delta E}} \quad (8)$$

However, this approach does not eliminate the issue of traditional single-molecule orbital-based approaches (typically performed in standard quantum chemistry programs) which, as noted above, overestimate polarization due to Coulomb interactions with neighboring molecules;[33] note that this can be eliminated using periodic boundary conditions.

Donor−Acceptor Strength and Bridging Groups. DBA molecules have exquisitely tunable single-molecule (hyper)-polarizabilities which depend on the strength of the donor/acceptor units and type of bridging group connecting them. Since, as shown above, DBA-based materials can exhibit excellent dielectric properties, it is of interest to investigate how changing donor/acceptor units and type of bridging group affect the dielectric response. In Figure 4A, the structures of the various DBA-based materials, labeled **1**−**4**, are shown. Monolayer **1** is identical to DA in the previous section. Monolayers **2** and **3** replace the second C═C in 1 with C−C and N═N bonds, respectively. Monolayer **4** changes the donor unit to $N(CH_3)_2$ and replaces the single NO_2 group with two C≡N groups: both substitutions have stronger donor or acceptor properties. Figure 4B shows optical and static dielectric constants for monolayers **1**−**4**. In monolayer **2**, breaking π conjugation eliminates donor−acceptor dielectric enhancement reducing the optical and static dielectric constants. Exchanging C═C for N═N in monolayer **3** increases the static dielectric constant, analogous to (hyper)-polarizability enhancement seen in DBA materials with identical substitution.[68] Insertion of stronger donor/acceptor units in monolayer **4** results in a small increase in optical and static dielectric constants. Since monolayer **4**'s substituents are more electron-rich than those of monolayer **1**, it is likely that this small increase in dielectric response is a result of increased charge density. These results show, as with molecular (hyper)polarizability and bulk linear/nonlinear optical susceptibility, that dielectric response can be broadly tuned in DBA materials via the donor and acceptor units and bridging groups.

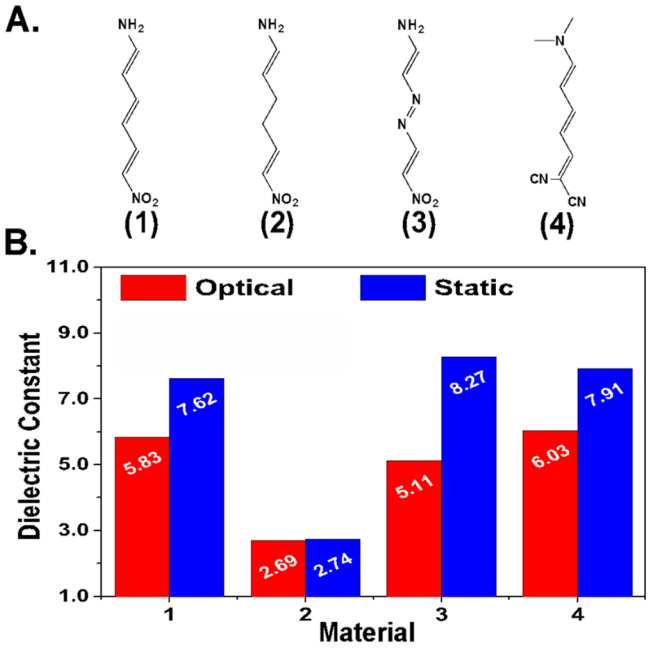

Figure 4. First-principles DFT computation of the optical and static dielectric constants of monolayers assembled from the indicated DBA molecules. (A) Chemical structures of DBA molecules **1**−**4**. (B) Optical (red bars) and static (blue bars) dielectric constants of the monolayers based on molecules **1**−**4**. The unit cell contains one molecule and has dimensions of 5.00 × 5.00 × 30.0 Å. The applied electric fields are parallel to the z axis and have a strength of $\pm 5.14 \times 10^8$ V/m A k-point sampling scheme of 2 × 2 × 1 is used for each material.

Squaraines. Substances with large dipole moments, such as organic ferroelectrics, can exhibit large dielectric constants.[69] In organic ferroelectric crystals, ordered dipole moments induce a significant dielectric response in the ferroelectric state, while significantly lower dielectric constants are achieved when the dipole moments are unaligned.[70,71] A reliable way to induce net dipole moments is by utilizing self-assembly to create energetically favorable interactions between the surface and adsorbing molecules. For instance, a surface with a positive charge could attract negatively charged acceptor groups of a DBA molecule to create a monolayer of DBA molecules oriented in the same direction.

Squaraine molecules have large optical responses and can be configured to act as covalently bonded donor−acceptor−donor (DAD) species.[72,73] In Figure 5A, a squaraine building block is shown with three possible substituent groups. The central C_4 squaric acid core acts as a powerful π-accepting group, and the two trans phenylene rings can act as donating or accepting groups depending on substituents. For clarity, we label squaraine with one squaric acid group as 1-Sq.-X_1X_2 with X_1 and X_2 representing different substituent groups on each

DOI: 10.1021/jacs.5b03301
J. Am. Chem. Soc. 2015, 137, 7189−7196

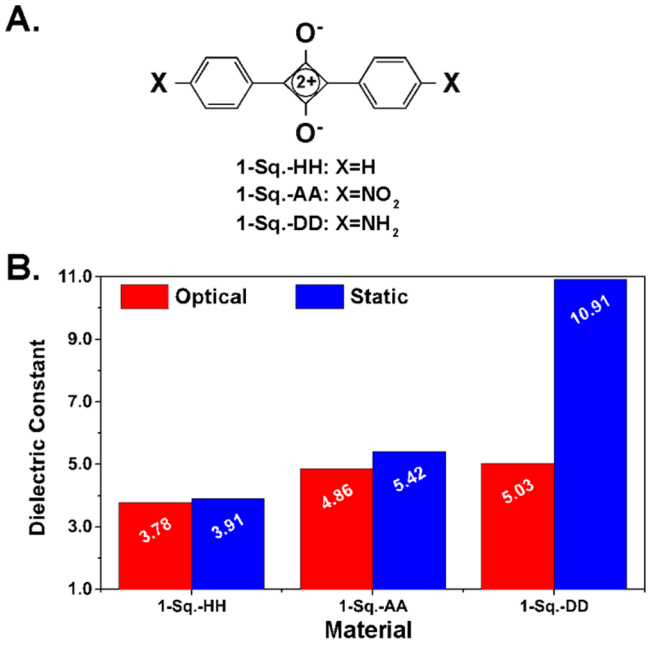

Figure 5. First-principles DFT computation of the optical and static dielectric constants of the indicated squaraine-based monolayer materials. Here the X-X vector is aligned perpendicular to the monolayer plane. (A) Chemical structure of substituted squaraines. (B) Optical (red bars) and static (blue bars) dielectric constants of the indicated substituted squaraines. The unit cell contains one molecule and has dimensions of 6.2 × 5.1 × 40.0 Å. The applied electric fields are parallel to the z axis and have a strength of $\pm 5.14 \times 10^8$ V/m. A k-point sampling scheme of 2 × 2 × 1 is used for each material.

phenylene ring. For instance, two hydrogen substituents on the phenylene rings is labeled as 1-Sq.-HH. Similarly, squaraines with NO_2 (acceptor) and NH_2 (donor) substituents are labeled 1-Sq.-AA and 1-Sq.-DD, respectively. In Figure 5B, optical and static dielectric responses are presented for monolayers fabricated from three substituted squarine molecules. Monolayers composed of building blocks 1-Sq.-HH and 1-Sq.-AA have lower computed dielectric constants than those of 1-Sq.-DD. This likely reflects the weak donor characteristics of H, and NO_2 acts as a strong acceptor. The larger dielectric constant of the 1-Sq.-AA-based monolayers versus those of 1-Sq.-HH may arise from the greater electron count, similar to what was seen in AH above. Monolayers of 1-Sq.-DD have a remarkable static dielectric constant that is essentially twice the optical dielectric constant. Due to the small molecular length and large dielectric constant, 1-Sq.-DD monolayers are predicted to have a capacitance of $C = 6.99$ μF/cm^2, 5× larger than that of current "champion" organic gate dielectric materials.[15]

From the above results it can be seen that proceeding from D−A to D−A−D molecules accrues further enhancement of monolayer dielectric performance. Furthermore, it is not necessary to halt at this point, and in Scheme 1, 1-Sq.-HH is catenated by appending one (2-Sq.-HH) or two (3-Sq.-HH) additional squaric acid units, capped with a corresponding donor group. Table 3 summarizes the optical and static dielectric constants of extended squaraines substituted with H (HH) or NH_2 (DD). In both the HH and DD substituted monolayers, the dielectric response increases with additional squaric acid groups. The DD substituted structures retain the largest dielectric constants, and the static dielectric constants

Scheme 1

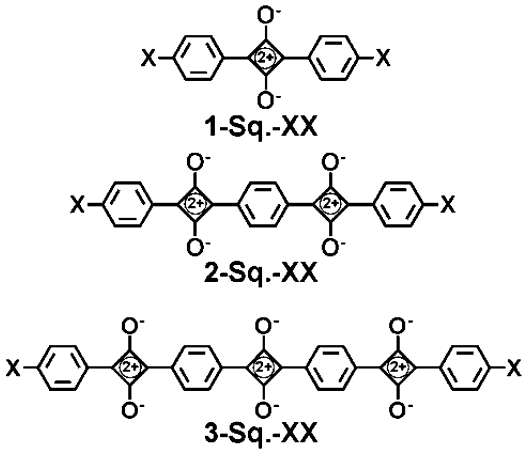

Table 3. Static and Optical Dielectric Constants of Monolayers Fabricated from Squaraine-Based Building Blocks 1-Sq.-XX, 2-Sq.-XX, and 3-Sq.-XX

	dielectric constant		capacitance (μF/cm^2)	
material	ε_o [a]	ε_s [b]	C_o [c]	C_s [d]
1-Sq.-HH	3.78	3.91	2.68	2.77
1-Sq.-DD	5.03	10.91	3.22	6.98
2-Sq.-HH	5.82	6.10	2.55	2.67
2-Sq.-DD	7.33	14.59	3.00	5.97
3-Sq.-HH	7.91	8.34	2.52	2.66
3-Sq.-DD	9.68	19.72	2.94	5.99

[a]Optical dielectric constant. [b]Static dielectric constant. [c]Optical frequency capacitance. [d]Static frequency capacitance of a monolayer.

remain nearly twice that of the optical dielectric constants. Note also that the 3-Sq.-DD-based material has the largest calculated dielectric constant, however, it has a slightly smaller capacitance than the 1-Sq.-DD-derived monolayer due to its increased thickness ($C = 5.99$ μF/cm^2). This result highlights a possible ceiling in capacitance values for organic dielectrics. Although the 3-Sq.-DD monolayer achieves a remarkable dielectric response, it shows capacitance losses due to increased monolayer thickness. Moving forward, to obtain higher capacitances organic dielectrics must remain thin (∼5.0 nm) while simultaneously increasing the dielectric response and maintaining close packing of the molecular constituents.

Model Validation. While the present model has been applied to many inorganic and, more recently, to limited organic systems, it is still important to ensure the accuracy of this approach for highly polarizable materials. It is generally accepted that GGA functionals, including PBE, provide acceptable accuracy for many conjugated organic molecular materials.[74,75] Unfortunately, many plane-wave codes have just recently begun to implement hybrid functionals into their suite of functionals, since traditional functionals such as LDA and GGA have typically proven adequate for the vast majority of materials studied. This delayed adoption of standard density functional methods seen in orbital-based packages, such as B3LYP, has limited optimization of hybrid functionals for plane-wave based methods. HSE,[76] a range-separated hybrid functional, has demonstrated excellent performance in computing a wide array of electronic structure properties [77] and is implemented in the QUANTUMESPRESSO software package. Thus, our PBE calculations were benchmarked against

DOI: 10.1021/jacs.5b03301
J. Am. Chem. Soc. 2015, 137, 7189−7196

identical calculations performed using the HSE functional, and the results are shown in Figure 6. We compare only two

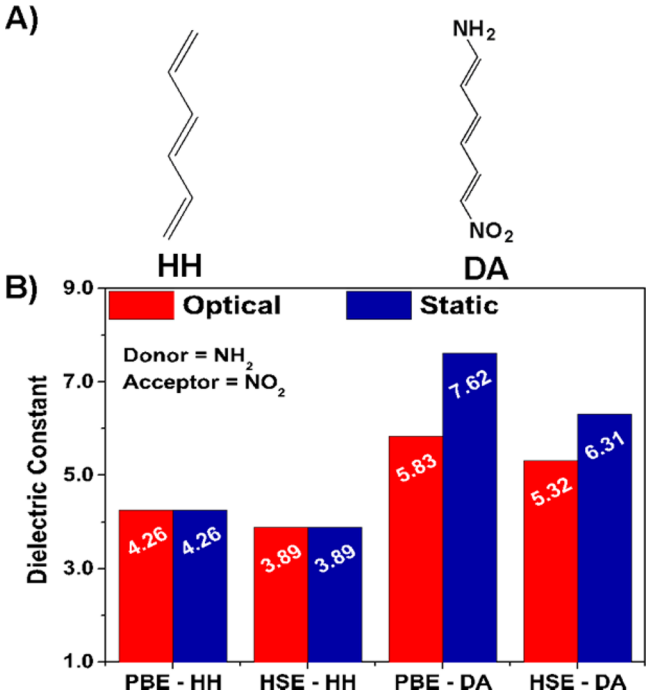

Figure 6. First-principles DFT calculation of optical and static dielectric constant of unsubstituted and substituted polyacetylene based monolayers. Here the molecular long axes are aligned perpendicular to the monolayer plane. (A) Chemical structures of the molecular constituents used for model validation. (B) Optical (red bars) and static (blue bars) dielectric constants of unsubtituted polyacetylene and polyacetylene substituted with NH_2 and NO_2 using PBE and HSE functionals. The unit cell contains one molecule and has dimensions of 5.0 × 5.0 × 40.0 Å. The applied electric fields are parallel to the z axis and have a strength of $\pm 5.14 \times 10^8$ V/m. A k-point sampling scheme of 2 × 2 × 1 is used for each material.

polyene compounds, HH and DA, due to prodigious computational demands associated with the HSE functional. As an example, a single HSE self-consistent field (SCF) calculation requires 10× more computational time than an equivalent PBE calculation. As expected, HSE predicts a somewhat lower dielectric response than PBE. PBE and other GGA methods are known to overestimate polarization in conjugated organic materials.[77,78] However, the same qualitative trends are observed using HSE, and there is reasonable agreement between them (20.0% variance). Due to the non-negligible overestimation of polarization, we caution that all computed dielectric constants are to some degree upper bounds for experimental values.

A hurdle in benchmarking dielectric calculations against experimental data is the paucity of reliable dielectric measurements on molecular thin films. Such measurements are sensitive to materials properties such as surface coverage and molecular orientation. Without knowing these details, it is difficult to make direct comparisons between theory and experiment. Another complication arises in multilayers when using standard parallel plate capacitor model, eq 9, to compute the dielectric constant:

$$\frac{d}{\varepsilon} = \sum_{i=1}^{x} \frac{d_i}{\varepsilon_i} \tag{9}$$

where d_i and ε_i are the thickness and dielectric constant, respectively, of component material i, d is the total thickness of the multilayer, and ε is the dielectric constant of the total multilayer. Using this model to calculate the dielectric constant of a single layer from the measured dielectric constant of the entire system is suspect unless the thickness and dielectric constant of each constituent layer is known. Specifically, the overall dielectric performance of a multicomponent system is determined predominantly by the layer having the smallest dielectric constant, meaning that small changes in local dielectric performance causes large changes in computed dielectric constant of the material using eq 9.

To compare computed and experimental dielectric constants of a molecular monolayer in a multicomponent system (e.g., V-SAND),[39,79] the smallest dielectric constant material is the controlling entity. If this effect is not taken into account, then meaningful comparisons between experiment and computation cannot be made. Two highly polarizable systems, V-SAND 1 and V-SAND 2, have experimentally determined dielectric constants[30,39] for monolayers of polarizable chromophores shown in Figure 7. Table 4 contains experimental and

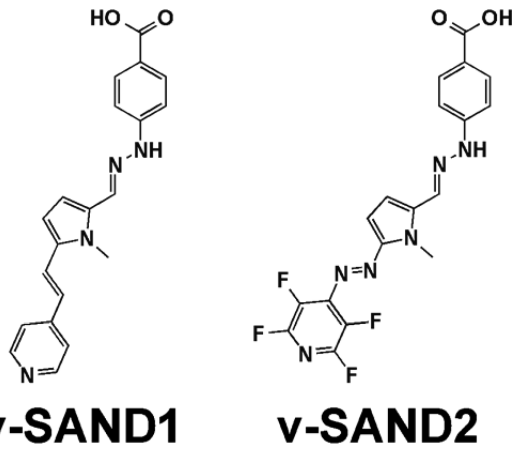

Figure 7. Chemical structures of vapor-deposited molecular dielectrics for comparing calculated and experimental dielectric properties.

Table 4. Computed and Experimental Static Dielectric Constant Values for V-SAND 1 and V- SAND 2

material	calculated ε^a	experimental ε^b
v-SAND 1	6.5	4.0−11.0
v-SAND 2	7.0	9.0−12.4

[a]Calculation performed assuming an applied electric field of $\pm 5.14 \times 10^8$ V/m and a surface coverage of 2.5 molecules/nm^2. [b]Values are from ref 9.

computed static dielectric constants at low frequency ($\omega < 10^6$ Hz). In V-SAND systems, the smallest dielectric constant layer originates from the ∼10 Å native SiO_2 film, ε = 3.90, coating the Si electrode, which makes extracting precise experimental film dielectric constants necessarily uncertain. However, comparisons between experiment and computation can reveal whether computed values are reasonable for these molecular monolayers and identify trends among dielectric films. Note that the computed V-SAND dielectric constants of

DOI: 10.1021/jacs.5b03301
J. Am. Chem. Soc. 2015, 137, 7189−7196

the indicated molecules are near the experimental values[30,39] and markedly higher than typical organic materials. Note also that these calculations assume a surface coverage of 2.5 molecules/nm^2 as found in experimental work on similar systems[80−82] and perpendicular alignment of the molecular long axes to the surface. Higher surface coverages and different surface alignment have been reported in other sterically less encumbered self-assembled systems,[24] which would affect computed dielectric constants. The present comparison shows that our computed dielectric constants are reasonably accurate for the highly polarizable materials studied in this paper. Further characterization of molecular monolayer systems with other high-dielectric constant materials would allow better comparison between experiment and computation.

■ CONCLUSIONS

Using first-principles calculations with periodic boundary conditions, highly polarizable DBA molecules are shown to be ideal candidates for high-capacitance dielectric thin-film materials. Incorporating both terminal donor and acceptor substituents into conjugated molecular structures substantially increases the dielectric response—more than would be expected by considering the donor and acceptor units separately. This cooperative effect can be tuned by altering molecular bridge and the donating or accepting strengths of the substituents. Dielectric enhancement in DBA materials is increased in stronger electric fields, a behavior reminiscent of enhanced nonlinear responses in high-hyperpolarizability molecules.[83] These findings suggest that molecular polarizability alone is not a proper metric of dielectric performance since it cannot incorporate nonlinear behavior. Classical formalisms such as the Clausius−Mossotti description should be altered to include non-linear terms, which can be achieved by replacing polarizability with change in dipole moment. Molecular monolayers composed of highly polarizable molecules, such as donor-substituted squaraines, can achieve calculated molecular capacitances >6.0 μF/cm^2 and dielectric constants ≈20.0, significantly higher than traditional organic materials. Integrating DBA dielectrics into FET transistors offers the potential to dramatically enhance performance to rival or exceed that of HfO_2 while maintaining molecular characteristics that make organic transistors attractive for electronic devices.

■ AUTHOR INFORMATION

Corresponding Authors

*t-marks@northwestern.edu

*ratner@northwestern.edu

Notes

The authors declare no competing financial interest.

■ ACKNOWLEDGMENTS

The research was supported by the MRSEC program of NSF (DMR-1121262) through the Northwestern University Materials Research Center. H.M.H. is supported by the Department of Defense (DoD) through the National Defense Science and Engineering Graduate Fellowship (NDSEG) Program.

■ REFERENCES

(1) Kamyshny, A.; Magdassi, S. *Small* **2014**, *10*, 3515−3535.

(2) Liao, C.; Zhang, M.; Yao, M. Y.; Hua, T.; Li, L.; Yan, F. *Adv. Mater.*, **2014**; DOI: 10.1002/adma.201402625.

(3) Lin, P.; Yan, F. *Adv. Mater. (Weinheim, Ger.)* **2012**, *24*, 34−51.

(4) Sirringhaus, H. *Adv. Mater.* **2014**, *26*, 1319−1335.

(5) Boudreault, P.-L. T.; Hennek, J. W.; Loser, S.; Ponce Ortiz, R.; Eckstein, B. J.; Facchetti, A.; Marks, T. J. *Chem. Mater.* **2012**, *24*, 2929−2942.

(6) Usta, H.; Risko, C.; Wang, Z.; Huang, H.; Deliomeroglu, M. K.; Zhukhovitskiy, A.; Facchetti, A.; Marks, T. J. *J. Am. Chem. Soc.* **2009**, *131*, 5586−5608.

(7) Ponce Ortiz, R.; Herrera, H.; Seoane, C.; Segura, J. L.; Facchetti, A.; Marks, T. J. *Chemistry* **2012**, *18*, 532−543.

(8) Kang, B.; Lee, W. H.; Cho, K. *ACS Appl. Mater. Interfaces* **2013**, *5*, 2302−2315.

(9) Kim, Y.-H.; Yoo, B.; Anthony, J. E.; Park, S. K. *Adv. Mater.* **2012**, *24*, 497−502.

(10) Ha, M.; Seo, J.-W. T.; Prabhumirashi, P. L.; Zhang, W.; Geier, M. L.; Renn, M. J.; Kim, C. H.; Hersam, M. C.; Frisbie, C. D. *Nano Lett.* **2013**, *13*, 954−960.

(11) Hennek, J. W.; Xia, Y.; Everaerts, K.; Hersam, M. C.; Facchetti, A.; Marks, T. J. *ACS Appl. Mater. Interfaces* **2012**, *4*, 1614−1619.

(12) Kim, S. H.; Hong, K.; Xie, W.; Lee, K. H.; Zhang, S.; Lodge, T. P.; Frisbie, C. D. *Adv. Mater.* **2013**, *25*, 1822−1846.

(13) Everaerts, K.; Emery, J. D.; Jariwala, D.; Karmel, H. J.; Sangwan, V. K.; Prabhumirashi, P. L.; Geier, M. L.; McMorrow, J. J.; Bedzyk, M. J.; Facchetti, A.; Hersam, M. C.; Marks, T. J. *J. Am. Chem. Soc.* **2013**, *135*, 8926−8939.

(14) Everaerts, K.; Zeng, L.; Hennek, J. W.; Camacho, D. I.; Jariwala, D.; Bedzyk, M. J.; Hersam, M. C.; Marks, T. J. *ACS Appl. Mater. Interfaces* **2013**, *5*, 11884−11893.

(15) Ha, Y.-G.; Everaerts, K.; Hersam, M. C.; Marks, T. J. *Acc. Chem. Res.* **2014**, *47*, 1019−1028.

(16) Heitzer, H. M.; Marks, T. J.; Ratner, M. A. *ACS Nano* **2014**, *8*, 12587−12600.

(17) Sangwan, V. K.; Ortiz, R. P.; Alaboson, J. M. P.; Emery, J. D.; Bedzyk, M. J.; Lauhon, L. J.; Marks, T. J.; Hersam, M. C. *ACS Nano* **2012**, *6*, 7480−7488.

(18) Sangwan, V. K.; Jariwala, D.; Filippone, S. A.; Karmel, H. J.; Johns, J. E.; Alaboson, J. M. P.; Marks, T. J.; Lauhon, L. J.; Hersam, M. C. *Nano Lett.* **2013**, *13*, 1162−1167.

(19) Sangwan, V. K.; Jariwala, D.; Everaerts, K.; McMorrow, J. J.; He, J.; Grayson, M.; Lauhon, L. J.; Marks, T. J.; Hersam, M. C. *Appl. Phys. Lett.* **2014**, *104*, 083503.

(20) Sharma, V.; Wang, C.; Lorenzini, R. G.; Ma, R.; Zhu, Q.; Sinkovits, D. W.; Pilania, G.; Oganov, A. R.; Kumar, S.; Sotzing, G. A.; Boggs, S. A.; Ramprasad, R. *Nat. Commun.* **2014**, *5*, 4845.

(21) DiBenedetto, S. A.; Facchetti, A.; Ratner, M. A.; Marks, T. J. *J. Am. Chem. Soc.* **2009**, *131*, 7158−7168.

(22) DiBenedetto, S. A.; Facchetti, A.; Ratner, M. A.; Marks, T. J. *Adv. Mater.* **2009**, *21*, 1407−1433.

(23) Rampi, M.; Schueller, O.; Whitesides, G. *Appl. Phys. Lett.* **1998**, *72*, 1781−1783.

(24) Slowinski, K.; Chamberlain, R. V.; Miller, C. J.; Majda, M. *J. Am. Chem. Soc.* **1997**, *119*, 11910−11919.

(25) Klauk, H.; Zschieschang, U.; Pflaum, J.; Halik, M. *Nature* **2007**, *445*, 745−748.

(26) Ulman, A. *Chem. Rev.* **1996**, *96*, 1534−1554.

(27) Yoon, M. H. *Proc. Natl. Acad. Sci. U. S. A.* **2005**, *102*, 4678−4682.

(28) Yoon, M.-H.; Kim, C.; Facchetti, A.; Marks, T. J. *J. Am. Chem. Soc.* **2006**, *128*, 12851−12869.

(29) Ting, G. G., II; Acton, O.; Ma, H.; Ka, J. W.; Jen, A. K. Y. *Langmuir* **2009**, *25*, 2140−2147.

(30) DiBenedetto, S. A.; Frattarelli, D. L.; Facchetti, A.; Ratner, M. A.; Marks, T. J. *J. Am. Chem. Soc.* **2009**, *131*, 11080−11090.

(31) Blythe, A. R.; Bloor, D. *Electrical Properties of Polymers*, 2nd ed.; Cambridge University Press: Cambridge, U.K., 2005.

(32) Heitzer, H. M.; Marks, T. J.; Ratner, M. A. *J. Am. Chem. Soc.* **2013**, *135*, 9753−9759.

(33) Natan, A.; Kuritz, N.; Kronik, L. *Adv. Funct. Mater.* **2010**, *20*, 2077−2084.

DOI: 10.1021/jacs.5b03301
J. Am. Chem. Soc. 2015, 137, 7189−7196

(34) Romaner, L.; Heimel, G.; Ambrosch-Draxl, C.; Zojer, E. *Adv. Funct. Mater.* **2008**, *18*, 3999−4006.
(35) Shi, N.; Ramprasad, R. *Appl. Phys. Lett.* **2006**, *89*, 102904.
(36) Pilania, G.; Ramprasad, R. *J. Mater. Sci.* **2012**, *47*, 7580−7586.
(37) Ramprasad, R.; Shi, N. *Phys. Rev. B* **2005**, *72*, 052107−052101.
(38) Yu, L.; Ranjan, V.; Nardelli, M.; Bernholc, J. *Phys. Rev. B* **2009**, *80*, 165432.
(39) DiBenedetto, S. A.; Frattarelli, D.; Ratner, M. A.; Facchetti, A.; Marks, T. J. *J. Am. Chem. Soc.* **2008**, *130*, 7528−7529.
(40) Facchetti, A.; Hutchison, G. R.; Keinan, S.; Ratner, M. A. *Inorg. Chim. Acta* **2004**, *357*, 3980−3990.
(41) Albinsson, B.; Eng, M. P.; Pettersson, K.; Winters, M. U. *Phys. Chem. Chem. Phys.* **2007**, *9*, 5847−5864.
(42) Bredas, J. L. *J. Chem. Phys.* **1985**, *82*, 3808−3811.
(43) Bredas, J. L.; Adant, C.; Tackx, P.; Persoons, A.; Pierce, B. M. *Chem. Rev.* **1994**, *94*, 243−278.
(44) Kanis, D. R.; Ratner, M. A.; Marks, T. J. *Chem. Rev.* **1994**, *94*, 195−242.
(45) Albert, I. D. L.; Marks, T. J.; Ratner, M. A. *Chem. Mater.* **1998**, *10*, 753−762.
(46) Dehu, C.; Meyers, F.; Bredas, J. L. *J. Am. Chem. Soc.* **1993**, *115*, 6198−6206.
(47) Verbiest, T.; Houbrechts, S.; Kauranen, M.; Clays, K.; Persoons, A. *J. Mater. Chem.* **1997**, *7*, 2175−2189.
(48) Davis, W. B.; Svec, W. A.; Ratner, M. A.; Wasielewski, M. R. *Nature* **1998**, *396*, 60−63.
(49) Wiberg, J.; Guo, L.; Pettersson, K.; Nilsson, D.; Ljungdahl, T.; Martensson, J.; Albinsson, B. *J. Am. Chem. Soc.* **2007**, *129*, 155−163.
(50) Kilsa, K.; Kajanus, J.; Macpherson, A. N.; Martensson, J.; Albinsson, B. *J. Am. Chem. Soc.* **2001**, *123*, 3069−3080.
(51) Nitzan, A. *Annu. Rev. Phys. Chem.* **2001**, *52*, 681−750.
(52) Nitzan, A.; Ratner, M. A. *Science* **2003**, *300*, 1384−1389.
(53) Mishra, A.; Ma, C.-Q.; Bäuerle, P. *Chem. Rev.* **2009**, *109*, 1141−1276.
(54) Shi, N.; Ramprasad, R. *J. Computer-Aided Mater. Des.* **2007**, *14*, 133−139.
(55) Natan, A.; Zidon, Y.; Shapira, Y.; Kronik, L. *Phys. Rev. B* **2006**, *73*, 193310.
(56) Giannozzi, P.; Baroni, S.; Bonini, N.; Calandra, M.; Car, R.; Cavazzoni, C.; Ceresoli, D.; Chiarotti, G. L.; Cococcioni, M.; Dabo, I.; Dal Corso, A.; de Gironcoli, S.; Fabris, S.; Fratesi, G.; Gebauer, R.; Gerstmann, U.; Gougoussis, C.; Kokalj, A.; Lazzeri, M.; Martin-Samos, L.; Marzari, N.; Mauri, F.; Mazzarello, R.; Paolini, S.; Pasquarello, A.; Paulatto, L.; Sbraccia, C.; Scandolo, S.; Sclauzero, G.; Seitsonen, A. P.; Smogunov, A.; Umari, P.; Wentzcovitch, R. M. *J. Phys.: Condens. Matter* **2009**, *21*, 395502.
(57) Perdew, J.; Burke, K.; Ernzerhof, M. *Phys. Rev. Lett.* **1996**, *77*, 3865−3868.
(58) Shi, N.; Ramprasad, R. *Phys. Rev. B* **2007**, 75.
(59) Champagne, B.; Jacquemin, D.; André, J.-M.; Kirtman, B. *J. Phys. Chem. A* **1997**, *101*, 3158−3165.
(60) McDowell, S. A. C.; Amos, R. D.; Handy, N. C. *Chem. Phys. Lett.* **1995**, *235*, 1−4.
(61) Heyd, J.; Scuseria, G. E. *J. Chem. Phys.* **2004**, *121*, 1187.
(62) Meyer, B.; Vanderbilt, D. *Phys. Rev. B* 2001, *63*.
(63) Vila, F. D.; Strubbe, D. A.; Takimoto, Y.; Andrade, X.; Rubio, A.; Louie, S. G.; Rehr, J. J. *J. Chem. Phys.* **2010**, *133*, 034111.
(64) Labello, N. P.; Ferreira, A. M.; Kurtz, H. A. *J. Comput. Chem.* **2005**, *26*, 1464−1471.
(65) Brown, E. C.; Marks, T. J.; Ratner, M. A. *J. Phys. Chem. B* **2008**, *112*, 44−50.
(66) Von Hippel, A. R. *Dielectric Materials and Applications*; Artech House on Demand: London, 1995.
(67) Schatz, G. C.; Ratner, M. A. *Quantum Mechanics in Chemistry*; Dover Publications, 2002.
(68) Tillman, N.; Ulman, A.; Elman, J. F. *Langmuir* **1990**, *6*, 1512−1518.
(69) Horiuchi, S.; Tokura, Y. *Nat. Mater.* **2008**, *7*, 357−366.
(70) Tokura, Y.; Koshihara, S.; Iwasa, Y.; Okamoto, H.; Komatsu, T.; Koda, T.; Iwasawa, N.; Saito, G. *Phys. Rev. Lett.* **1989**, *63*, 2405−2408.
(71) Okamoto, H.; MITANI, T.; Tokura, Y.; Koshihara, S.; Komatsu, T.; Iwasa, Y.; Koda, T.; Saito, G. *Phys. Rev., B Condens. Matter* **1991**, *43*, 8224−8232.
(72) Baettig, P.; Spaldin, N. A. *Appl. Phys. Lett.* **2005**, *86*, 012505.
(73) Resta, R.; Vanderbilt, D. *Theory of Polarization: A Modern Approach*; Springer: Berlin, Heidelberg, 2007; Vol. *105*, pp 31−68.
(74) Sekino, H.; Maeda, Y.; Kamiya, M.; Hirao, K. *J. Chem. Phys.* **2007**, *126*, 014107.
(75) Janesko, B. G. *J. Chem. Phys.* **2011**, *134*, 184105.
(76) Heyd, J.; Scuseria, G. E.; Ernzerhof, M. *J. Chem. Phys.* **2006**, *124*, 219906.
(77) Henderson, T. M.; Paier, J.; Scuseria, G. E. *Phys. Status Solidi B* **2010**, *248*, 767−774.
(78) Brothers, E. N.; Izmaylov, A. F.; Normand, J. O.; Barone, V.; Scuseria, G. E. *J. Chem. Phys.* **2008**, *129*, 011102.
(79) DiBenedetto, S. A.; Frattarelli, D. L.; Facchetti, A.; Ratner, M. A.; Marks, T. J. *J. Am. Chem. Soc.* **2009**, *131*, 11080−11090.
(80) Yitzchaik, S.; Di Bella, S.; Lundquist, P. M.; Wong, G. K.; Marks, T. J. *J. Am. Chem. Soc.* **1997**, *119*, 2995−3002.
(81) Yitzchaik, S.; Marks, T. J. *Acc. Chem. Res.* **1996**, *29*, 197−202.
(82) Albert, I. D. L.; Marks, T. J.; Ratner, M. A. *J. Am. Chem. Soc.* **1997**, *119*, 6575−6582.
(83) Alyar, H. *Rev. Adv. Mater. Sci.* **2013**, *34*, 79−87.

DOI: 10.1021/jacs.5b03301
J. Am. Chem. Soc. 2015, 137, 7189−7196